Targeting the adenosinergic system: Ligand binding kinetics and label-free assays for the study of SLC29A1 transporter and A2B adenosine receptor

Vlachodimou A.

Citation

Cover Page

Universiteit Leiden

Leiden University
Repository

Author: Vlachodimou, A.
Title: Targeting the adenosinergic system: Ligand binding kinetics and label-free assays for the study of SLC29A1 transporter and A2B adenosine receptor
Issue Date: 2020-11-04

Affinity, binding kinetics and functional characterization of draflazine analogues for human Equilibrative Nucleoside Transporter 1 (SLC29A1)
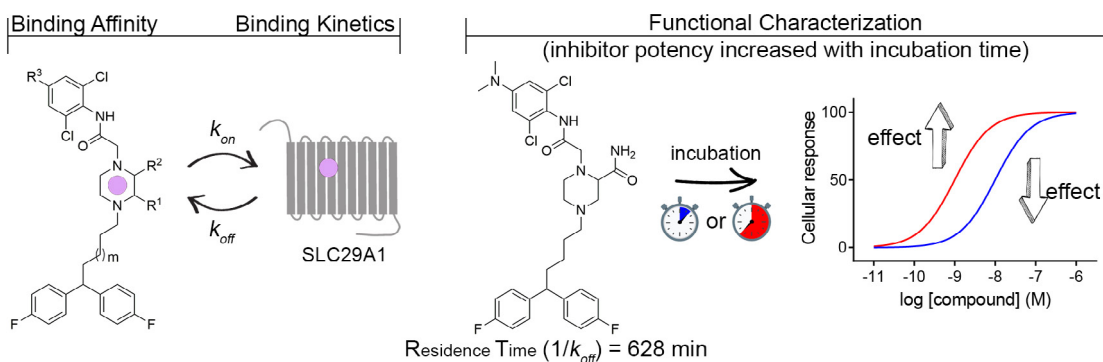
Anna Vlachodimou, Konstantina Konstantinopoulou,
Adriaan P. IJzerman, and Laura H. Heitman

Abstract

In the last decade it has been recapitulated that receptor-ligand binding kinetics is a relevant additional parameter in drug discovery to improve *in vivo* drug efficacy and safety. The equilibrative nucleoside transporter-1 (ENT1, SLC29A1) is an important drug target, as transporter inhibition is a potential treatment of ischemic heart disease, stroke, and cancer. Currently, two non-selective ENT1 inhibitors (dilazep and dipyridamole) are on the market as vasodilators. However, their binding kinetics are unknown; moreover, novel, more effective and selective inhibitors are still needed. Hence, this study focused on the incorporation of binding kinetics for finding new and improved ENT1 inhibitors.

We developed a radioligand competition association assay to determine the binding kinetics of ENT1 inhibitors with four chemical scaffolds (including dilazep and dipyridamole). The kinetic parameters were compared to the affinities obtained from a radioligand displacement assay. Three of the scaffolds presented high affinities with relatively fast dissociation kinetics, yielding short to moderate residence times (RTs) at the protein (1-44 min). While compounds from the fourth scaffold, *i.e.* draflazine analogues, also had high affinity, they displayed significantly longer RTs, with one analogue (**4**) having a RT of over 10 h. Finally, a label-free assay was used to evaluate the impact of divergent ENT1 inhibitor binding kinetics in a functional assay. It was shown that the potency of compound **4** increased with longer incubation times, which was not observed for draflazine, supporting the importance of long RT for increased target-occupancy and effect.

In conclusion, our research shows that high affinity ENT1 inhibitors show a large variation in residence times at this transport protein. As a consequence, incorporation of binding kinetic parameters adds to the design criteria and may thus result in a different lead compound selection. Taken together, this kinetic approach could inspire future drug discovery in the field of ENT1 and membrane transport proteins in general.

Introduction

Nucleoside Transporters (NTs) belong to the Solute Carrier (SLC) family and are transmembrane proteins that act as the cell's gatekeepers for purine and pyrimidine nucleobases and nucleosides[1]. They play a vital role in many cellular processes including protein synthesis, cell replication, signal transduction, energy source and metabolism[2,3]. The NTs are classified into two major classes, sodium-dependent concentrative transporters (CNTs; SLC28) and equilibrative (ENTs; SLC29) NTs .

Human ENT1 (hENT1; SLC29A1) is the best-studied SLC29 member[4]. It is expressed throughout the human body in tissues such as gastrointestinal tract, vascular endothelium, brain, while its expression levels vary between tissues[5,6]. ENT1 is known to have 11 transmembrane (TM) domains, and the region between TM domains 3 and 6 is responsible for the binding of reference inhibitors, such as dilazep, and S-(4-Nitrobenzyl)-6-thioinosine (NBTI), which was recently confirmed by the first crystal structure of this protein[7].

ENT1 has been extensively studied as a target for nucleoside analogue drugs, which are transported inside the cell, and used in the treatment of cancer or viral infections. Examples are gemcitabine[8], and ribavirin[9]. However, inhibition of ENT1 has also been proven to be a promising therapeutic strategy. Adenosine is a purine nucleoside and the main substrate of ENT1, as well as the endogenous ligand of a G protein-coupled receptor (GPCR) subfamily, the adenosine receptors (*i.e.* A_1, A_{2A}, A_{2B} and A_3). Inhibition of ENT1 modulates the extracellular concentration of adenosine leading to increased signaling via adenosine receptors, hence to a therapeutic effect. For example, draflazine has been shown to protect heart tissue against ischemia-induced damage, and its effect was attributed to the increased extracellular adenosine concentration[10]. Dilazep and dipyridamole, the two marketed ENT1 inhibitors, act as vasodilators via the same mechanism, however their effect is enhanced by inhibiting other targets, as they are non-selective[11,12].

In the last two decades target binding kinetics has emerged as an important parameter in drug discovery. Since then a plethora of research on association and dissociation rate constants, k_{on} and k_{off}, respectively, has shown that *in vivo* efficacy is often associated to optimized binding kinetic parameters of the ligand[13,14]. Association rate has been found essential for high target occupancy, as it increases rebinding to the target[15]. In addition, it has been proven important for drug selectivity towards different targets, resulting to a higher drug safety[16]. Concerning k_{off}, its optimization leads to the tuning of target residence time (RT) and as a result to a favorable duration of action and efficacy[17]. Although the binding kinetics of some ENT1 inhibitors have been studied[18], they have yet to be incorporated in drug discovery efforts, *i.e.* by constructing structure-kinetics (SKR) next to structure-affinity relationships (SAR).

In this study, we report the biological evaluation of ENT1 reference inhibitors from four chemical scaffolds, *i.e.* NBTI, dilazep, dipyridamole and draflazine (Figure 1), as well as of nine draflazine analogues. For the purposes of this work [³H]NBTI

binding was characterized and a competition association assay was developed and validated for the determination of inhibitor target binding kinetics. In addition, kinetically diverse inhibitors were functionally evaluated in a label-free impedance-based assay, where it was shown that divergent binding kinetics resulted in distinct functional inhibition. Taken together, we established both structure-affinity and structure-kinetics relationships (SAR and SKR) for ENT1 inhibitors, from which one of the draflazine analogues emerged as an inhibitor with very slow dissociation rate and a prolonged functional effect compared to the other inhibitors.
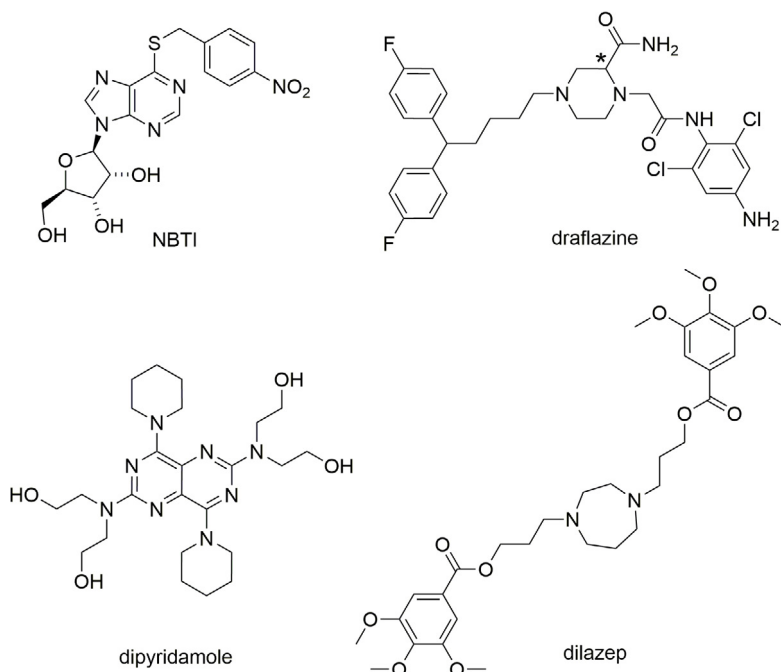
Figure 1: Chemical structures of the four reference hENT1 inhibitors used in this study. Draflazine is the (-)-enantiomer and the asymmetric carbon atom is indicated by *.

Results

Characterization of [³H]NBTI binding

The affinity of [³H]NBTI for the hENT1 transporter on erythrocyte membranes was determined with saturation binding experiments (Figure 2A). Transporter binding was saturable and characterized by a K_D of 1.1 nM and a B_{max} of 31 pmol/mg (Table 1). In addition, homologous displacement experiments with [³H]NBTI resulted in a pK_i value of 9.24 for NBTI (Figure 2D, Table 1).

Figure 2: Characterization of [³H]NBTI binding to hENT1 transporters endogenously expressed on erythrocyte membranes at 10 °C. (A) Saturation analysis of [³H]NBTI binding. (B) Association and dissociation kinetics of 4 nM [³H]NBTI to and from hENT1 transporters. Data are expressed as percentage of specific [³H]NBTI binding. (C) Competition association assay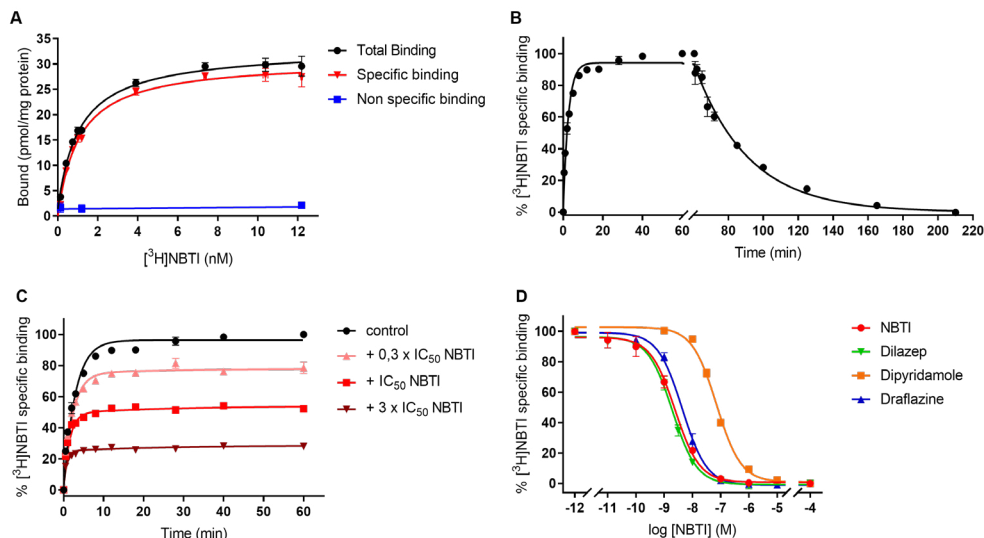 of [³H]NBTI (4 nM) in the absence or presence of 0.3x, 1x, and 3x IC_{50} of unlabeled NBTI. (D) Displacement of [³H]NBTI (4 nM) from hENT1 by non-labeled NBTI, dilazep, dipyridamole and draflazine. Data are shown as mean ± SEM from at least three independent experiments performed in duplicate.

Next to equilibrium radioligand binding assays, kinetic binding assays were performed to establish the association (k_{on}) and dissociation (k_{off}) rate constants of [³H]NBTI for the hENT1 transporter expressed on erythrocyte membranes (Figure 2B, Table 1). Equilibrium binding was reached in less than 15 min, while complete dissociation was reached within 150 min, as assessed by association and dissociation experiments best fitted with a one-phase model. As a result, k_{on}, k_{off} and RT values of 0.08 nM^{-1} min^{-1}, 0.036 min^{-1} and 28 min were calculated, respectively. From the aforementioned kinetic data the dissociation constant (kinetic K_D) was calculated and found to be 0.45 nM, which together with the equilibrium K_D obtained from saturation binding experiments indicated high affinity binding of [³H]NBTI for the hENT1 transporter.

Determination of the binding affinity of hENT1 inhibitors

Radioligand binding studies of 13 inhibitors were performed to determine their equilibrium binding affinity for the ENT1 transporter. All ligands were able to inhibit specific [³H]NBTI binding to ENT1 completely, in a competitive and concentration-

dependent manner. The reference marketed compounds displayed high affinities, with K_i values of 0.41 nM for dilazep and 14 nM for dipyridamole (Table 2). In contrast, draflazine and its analogues presented a greater range of affinities, ranging from 0.94 nM to 1133 nM for draflazine and compound **2**, respectively (Table 2).

Validation and optimization of the competition association assay

In order to determine the binding kinetics of all non-radiolabeled ligands of interest, a radioligand competition association assay was set up. The specific binding of radiolabeled NBTI was measured over a time course of 60 minutes, in the absence and presence of three different concentrations of unlabeled NBTI, *i.e.* 0.3, 1.0 and 3.0-fold its IC_{50} value as determined from the displacement assays (Figure 2C). By fitting the k_{on} and k_{off} values of [³H]NBTI binding into the "kinetics of competitive binding" model as described in the Materials and Methods section, the k_{on} and k_{off} values of the unlabeled NBTI were calculated to be 0.114 nM^{-1} min^{-1} and 0.051 min^{-1}, respectively (Table 1). As the k_{on} and k_{off} values obtained from this assay were in very good agreement with those from the classical association and dissociation assays, the competition association assay was deemed validated for determining unlabeled ligand's binding kinetics. Subsequently, a single concentration of NBTI (1.0-fold its IC_{50}) was assessed and found to result in similar binding kinetic values, *i.e.* 0.104 ± 0.014 nM^{-1} min^{-1} and 0.045 ± 0.001 min^{-1} for k_{on} and k_{off} respectively (data not shown). Consequently, the throughput of this competition association assay was increased, and it was decided to test other ligands at a concentration equal to 1.0-fold their IC_{50} only.

Determination of the binding kinetics of unlabeled hENT1 inhibitors

All the ligands with affinity values lower than 100 nM were evaluated in the competition association assay in order to determine their binding kinetic parameters, k_{on}, k_{off}, RT and K_D. Figure 3A presents the curves of the reference inhibitors dilazep and dipyridamole, which display similar, and shorter RTs compared to the radioligand [³H]NBTI (control curve), respectively. In Figure 3B, the graph obtained with draflazine and the long RT compound **4** is presented, where the incubation was increased to 3h as their residence time exceeded that of the radioligand. This resulted in a characteristic overshoot followed by a steady decrease to a lower equilibrium. Association rate constants of all ligands displayed a modest 8-fold range, *i.e.* 0.0016 nM^{-1} min^{-1} for compound **4** to 0.013 nM^{-1} min^{-1} for **1** and **6**. In contrast, dissociation rate constants exhibited a greater 101-fold range, with compounds **4** and **1** having the lowest and the highest values (0.0016 min^{-1} and 0.162 min^{-1}), respectively.

Table 1: Comparison of the affinity, dissociation constants and kinetic parameters of reference ENT1 inhibitor, NBTI, obtained with different radioligand binding assays performed on human erythrocyte membranes.

Assay	B_{max} (pmol/mg)	K_D (nM)	pK_i (K_i (nM))[a]	k_{on} (nM^{-1} min^{-1})	k_{off} (min^{-1})	RT (min)
Saturation binding	31 ± 0.9	1.1 ± 0.028	-	-	-	-
Displacement	-	-	9.24 ± 0.03 (0.57)	-	-	-
Association and dissociation	-	0.45 ± 0.05[b]	-	0.080 ± 0.007	0.036 ± 0.002	28 ± 1.4
Competition association	-	0.45 ± 0.06[b]	-	0.114 ± 0.014[c]	0.051 ± 0.003[c]	20 ± 1.3[c]

Values are mean ± SEM of at least three individual experiments performed in duplicate. [a]pK_i values were calculated from pIC_{50} values and the saturation K_D value using the ChengPrusoff equation: $K_i = IC_{50}$ / (1 + [radioligand] / K_D). [b]Kinetic K_D values determined by association and dissociation, and competition association assay, is defined as $K_D = k_{off}/k_{on}$. [c]The binding kinetics of unlabeled NBTI were determined by addition of 0.3-, 1- and 3-fold its IC_{50} value (as obtained from displacement assays).

Table 2. Affinity (pK_i, K_D) and kinetic parameters (k_{on}, k_{off}, RT) of reference ENT1 inhibitors and inhibitors **1 – 9**, sharing the draflazine scaffold.

cmpd	m	R¹	R²	R³	pK$_i$ (K$_i$ (nM))[a]	k$_{on}$ (nM⁻¹min⁻¹)	k$_{off}$ (min⁻¹)	RT (min)[b]	K$_D$ (nM)[c]
dilazep	-	-	-	-	9.39 ± 0.06 (0.41)	0.10 ± 0.00	0.023 ± 0.004	44 ± 7.6	0.22 ± 0.04
dipyridamole	-	-	-	-	7.85 ± 0.04 (14)	0.008 ± 0.001	0.082 ± 0.003	12 ± 0.5	10 ± 1.3
1	0	H	CONH₂	H	7.56 ± 0.05 (28)	0.013 ± 0.003	0.16 ± 0.04	6.2 ± 1.5	13 ± 4.7
2	0	H	CONHCH₃	H	5.95 ± 0.05 (1133)	n.d.[d]	n.d.	n.d.	n.d.
3	1	H	CONH₂	H	7.98 ± 0.05 (10)	0.009 ± 0.000	0.022 ± 0.001	46 ± 2.9	2.5 ± 0.2
draflazine*	1	H	CONH₂	NH₂	9.03 ± 0.08 (0.94)	0.010 ± 0.004	0.011 ± 0.004	88 ± 30	1.1 ± 0.6
4	1	H	CONH₂	N(CH₃)₂	7.33 ± 0.06 (47)	0.0016 ± 0.0002	0.0016 ± 0.0007	628 ± 294	1.0 ± 0.5
5	1	H	CONH₂	COCH₃	8.05 ± 0.08 (8.9)	0.007 ± 0.002	0.012 ± 0.001	83 ± 6.2	1.6 ± 0.4
6	0	CONH₂	H	H	8.09 ± 0.11 (8.2)	0.013 ± 0.002	0.055 ± 0.004	18 ± 1.3	4.2 ± 0.6
7	0	CONHCH₃	H	H	7.82 ± 0.09 (15)	0.004 ± 0.000	0.051 ± 0.002	20 ± 0.8	12 ± 0.8
8	1	CONH₂	H	H	8.27 ± 0.12 (5.4)	0.009 ± 0.001	0.014 ± 0.001	71 ± 5.1	1.6 ± 0.2
9	1	CONH₂	H	N(CH₃)₂	7.46 ± 0.05 (34)	0.003 ± 0.000	0.022 ± 0.003	46 ± 6.2	8.2 ± 1.7

Values represent the mean ± SEM of at least three individual experiments, performed in duplicate. [a]pK$_i$ values were calculated from pIC$_{50}$ values and the saturation K$_D$ value using the Cheng-Prusoff equation: K$_i$ = IC$_{50}$ / (1 + [radioligand] / K$_D$). [b]RT =1/k$_{off}$. [c]Kinetic K$_D$ values, defined as K$_D$ = k$_{off}$/k$_{on}$. [d]n.d. = not determined. *Draflazine is the (-)-enantiomer, as shown in Figure 1.
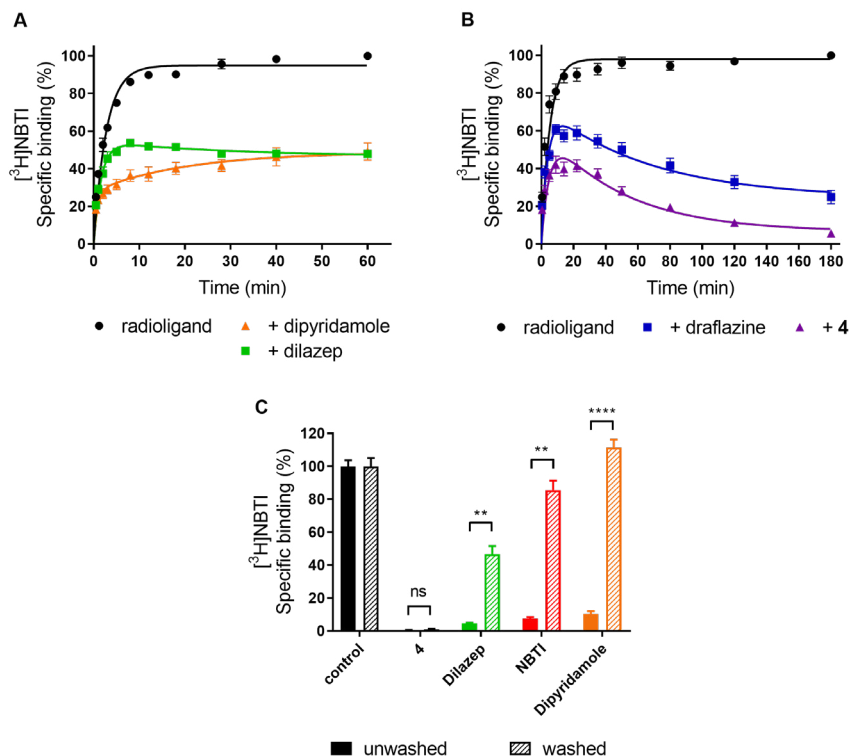
Figure 3: Evaluation of binding kinetics of reference compounds and the longest RT draflazine analogue at 10 °C. The assays have been performed on erythrocyte membranes with 4 nM of [³H]NBTI. (A) Competition association assay of [³H]NBTI to hENT1 transporter in the absence or presence of IC_{50} concentration of the reference ENT1 inhibitors dilazep and dipyridamole. (B) Competition association assay of [³H]NBTI to hENT1 transporter in the absence or presence of an IC_{50} concentration of draflazine and compound **4**. The duration of the measurement was increased to 3 h in order to more accurately assess compound **4**'s long RT. (C) Recovery of radioligand binding after washing. [³H]NBTI binding after 1 h pre-incubation with a 10 x IC_{50} concentration of ENT1 inhibitors followed by no (unwashed) or 4x (washed) washing. Data are shown as mean ± SEM from at least three independent experiments performed in duplicate. Statistical analysis between the unwashed and washed condition of each ligand were performed using parametric paired t-tests. ns p > 0.05, ** p ≤ 0.01, **** p ≤ 0.0001.

Structure-Affinity Relationships (SAR) and Structure-Kinetic Relationships (SKR) of draflazine analogues

In an effort to better compare the inhibitors tested and understand their interactions with the transporter, both SAR and SKR were drawn based on the affinities (K_i values) and the kinetic parameters (k_{on}, k_{off} values and RT), obtained from the equilibrium binding and competition association assays. Amongst the reference compounds, *i.e.* NBTI, dilazep, dipyridamole and draflazine, only draflazine presented a longer RT

(Table 1 and 2). Thus, the draflazine scaffold was selected for further binding kinetic characterization. To efficiently explore the SAR and SKR around the draflazine scaffold, nine draflazine analogues, with variation in the length of the carbon linker connecting the the piperazine and the (bis)fluorophenyl moieties, the position and type of substitution on the piperazine ring, and substituent on the 4-position of the 2,6 di-chloro phenyl ring were studied for their affinity. From these analogues, only eight showed sufficient affinity to warrant further characterization of their binding kinetics.

Compound **1** was taken as the starting point. Replacement of carboxamide at the R^2 with an methylamide (**2**) led to a decreased affinity. As a result, carboxamide was used as the R^2 substituent for compounds **3-5** and draflazine. Increasing the carbon chain length by 1 carbon (m=1; **3**) resulted in a moderate increase in affinity and a decrease in dissociation rate constant. Introducing an amine on the R^3 position (draflazine) increased the affinity, resulting in the highest affinity for hENT1 of all measured compounds. In addition, a modest increase in k_{on} and a 2-fold decrease in k_{off} was presented, yielding in an intermediate RT of 88 minutes. The SAR and SKR study continued with the di-substitution of the amine with methyl which led to compound **4**. Compound **4** showed a significantly lower affinity (50-fold) for ENT1 compared to draflazine, as well as a 6-fold and 7-fold decrease in k_{on} and k_{off}, respectively. However, due to the slow dissociation rate of compound **4**, no equilibrium was reached in this 60 min assay. As a consequence the derived pKi value is an underestimated apparent affinity. Compound **4**'s kinetic affinity K_D is therefore a better parameter, and no decrease of affinity was observed compared to draflazine. Compound **4** proved to be the longest RT (> 10 h) compound tested, while showing the lowest association rate constant. Subsequently, the introduction of an acetyl group (**5**) was investigated. Compared to draflazine, compound **5** showed a decrease in affinity of half a log unit, while no change was observed for RT strong decrease in RT, resulting in an intermediate RT of 83 minutes.

In addition to substitution of the R^2 position of the piperazine, the R^1 position was investigated. Compounds **6**, **7**, **8** and **9** were investigated as counterparts to **1**,**2**,**3** and **4** and the same trend was observed. In all cases, a linker of 4 carbons (m=1; **8** and **9**) and an carboxamide (**6**, **8** and **9**) instead of methylamide (**7**) resulted in higher affinities. Furthermore, by comparison of **1** and **6**, **3** and **8**, **4** and **9**, it is not clear if substitution with carboxamide on the R^1 or R^2 position of the piperazine moiety is crucial for longer RT. The study of draflazine, **4** and **9** reveals that para-substitution of the 2,6 di-chloro phenyl ring with an amine increased the RT.

Evaluation of binding kinetics in a washout assay

To further validate the findings of the competition association assay, a washout radioligand binding assay was developed as described under *Methods and Materials*. In this assay the recovery of radioligand binding before and after several wash-

centrifugation steps by incubation with NBTI, dilazep, dipyridamole and compound **4** with the transporter was investigated. Dipyridamole showed a complete recovery in radioligand binding after the wash-centrifugation steps, while for NBTI and dilazep a partial recovery was found (Figure 3C), indicating that these inhibitors were either entirely or partially washed from the transporter. On the contrary, pre-incubation with compound **4** completely prevented a recovery of radioligand binding, as no significant difference was observed between the washed and unwashed condition (0.94% and 0.15%, respectively, Figure 3C). Notably, in all cases the level of radioligand binding recovery was in agreement with the data from the competition association assay, *i.e.* the longer the RT time of the compounds tested, the smaller the recovery in radioligand binding measured after the washing steps (*i.e.* compound **4** < dilazep < NBTI < dipyridamole in both cases).
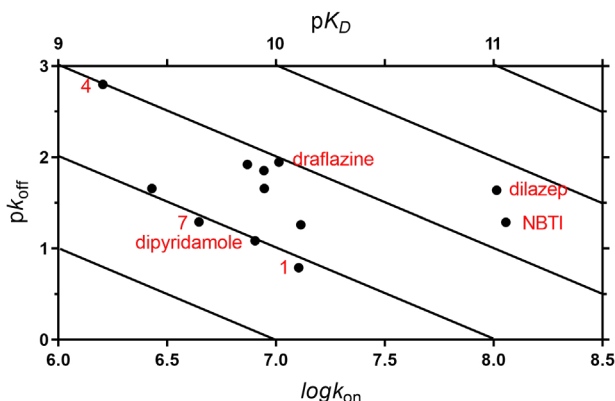
Kinetic map and Correlation plots

Figure 4: Kinetic map of all kinetically characterized inhibitors. The kinetically derived affinity (K_D) is represented by the diagonal parallel lines. The names/numbers of a few compounds are indicated in red next to the corresponding data point.

Next, we represented all compounds in a kinetic map to better illustrate the added value of determining structure-kinetic relationships (SKR), next to studying traditional structure-affinity-relationships (SAR) (Figure 4). In this map, the association (*x*-axis) and dissociation (*y*-axis) rate constants are plotted resulting in the kinetic affinity on the diagonal axis. As can be observed from this plot, two compounds on the same diagonal line have the same affinity for ENT1, but can have various combinations of association and dissociation rate constants. For example, compound **4** and NBTI have similar kinetic affinities (1.0 and 0.45 nM, respectively), however their k_{on} and k_{off} values differ by 71- and 32-fold, respectively. Furthermore, compounds may have an equal RT on ENT1, yet their affinity and association rates can differ a lot (e.g. NBTI and compound **7** have a RT of 20 min, while their affinity and k_{on} vary by

27- and 29-fold, respectively). Lastly, inhibitors could exhibit similar association rate constants, but different affinities due to divergent dissociation rate constants, like draflazine and compound **1**.
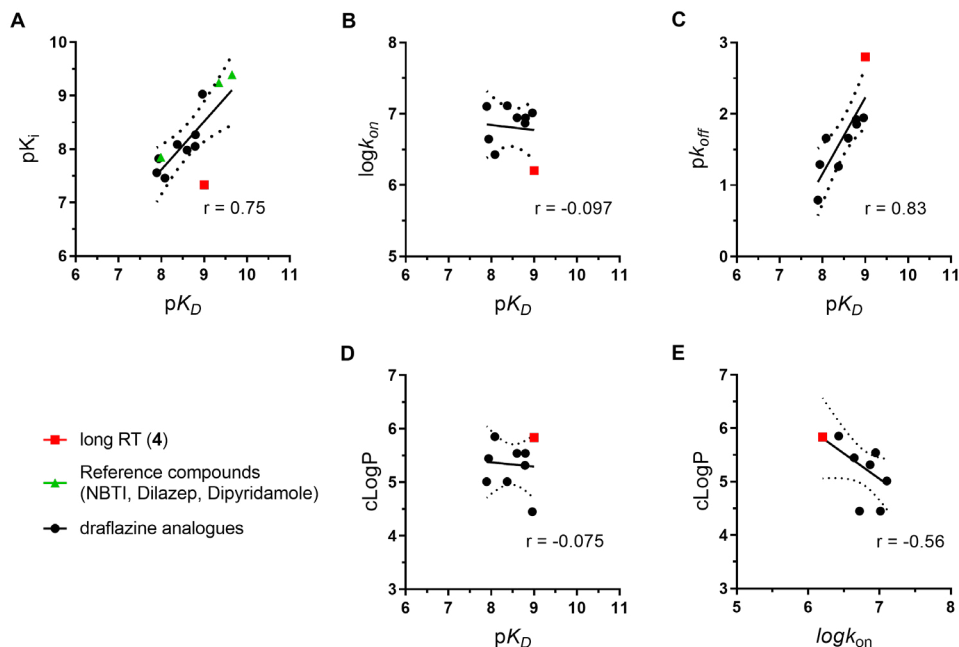

Figure 5: Correlation plots between affinity, kinetic parameters and lipophilicity. (A) Affinity determined from equilibrium displacement assays (pK$_i$) of all compound tested versus their kinetic affinity (pK$_D$) determined based on association (k_{on}) and dissociation (k_{off}) rate constants obtained from competition association assays. (B) Kinetic affinity (pK$_D$) of all draflazine analogues plotted against their association rate constants (logk_{on}), or (C) dissociation rate constants (pk$_{off}$). (D) Lipophility (cLogP values) of all draflazine analogues plotted against their kinetic affinity, or (E) association rate constants. The solid line corresponds to the linear regression of the data, the dotted line represents the 95% confidence interval for regression and the Pearson r coefficient is shown. Data used in the plots are detailed in Tables 1 and 2. Data are expressed as mean from at least three independent experiments performed in duplicate.

In order to get a better insight into the relationship between the different parameters obtained in this study, correlation plots were constructed (Figure 5). The affinity obtained from equilibrium radioligand binding assays (pK$_i$) for all compounds was plotted against the affinity calculated from the kinetic parameters (pK$_D$) and found to have a modest, yet significant correlation (r = 0.75, p = 0.0048). However, when the long RT compound (**4**; depicted by a red square in Figure 5A) was excluded, the two parameters were highly correlated (r = 0.92, p < 0.0001), suggesting that valid affinity values are best obtained through kinetic assays. Secondly, the association (logk_{on}) and dissociation (pk$_{off}$) rate constants of all draflazine analogues were plotted

against their kinetic affinity (pK_D) (Figure 4B, 4C). Here, only the pk_{off} was strongly correlated with kinetic affinity (r = 0.83, p = 0.0057), while this correlation was not observed with the equilibrium affinity (r = 0.61 and p = 0.084 for $logk_{on}$ vs pKi, r = 0.01 and p = 0.98 for pk_{off} vs pK_i; data not shown). Lastly, the lipophility (clogP) of all draflazine analogues was calculated, and it was not found to be significantly correlated with pK_D (r = -0.075, p = 0.85), $logk_{on}$ (r = -0.56, p = 0.09) (Figure 4D, 4E) or pk_{off} (r = 0.51, p = 0.13; data not shown).

Functional evaluation of binding kinetics for draflazine and compound 4

Finally, the large difference in RT of reference compound draflazine and its analogue **4**, and therefore the affinities established by 1h equilibrium (pK_i) or kinetic (K_D) radioligand binding assays, prompted us to investigate time-dependence in a functional assay. In short, increasing concentrations of the inhibitors were pre-incubated with U-2 OS cells for 30 min (Figure 6A,B) or 4 h (Figure 6C,D), followed by a 90 min incubation with $10^{-4.5}$ M adenosine. The latter induces activation of adenosine receptors, without which the effects of the ENT1 inhibitors cannot be observed. The area under the curve (AUC) of adenosine signaling was measured and found to be concentration-dependent for both inhibitors. Interestingly, the presence of compound **4** resulted in a left-ward shift of the adenosine effect with a longer pre-incubation time, while a small, if any, difference was observed with longer pre-incubation of draflazine (Figure 6E,F). As detailed in Table 3, the inhibitory effect of draflazine was slightly affected, yielding in an approximate 2-fold shift in IC_{50} value, while the potency of compound **4** was increased by about 47-fold. This suggests that an inhibitor with longer transporter residence time has an increased level of target occupancy over time, resulting in a higher potency.

Table 3: Potency (pIC_{50}) of ENT1 inhibitors draflazine and compound 4, determined by functional assay.

	pIC50 (IC50 (nM))	
	30 min pre	**4 h pre**
draflazine	8.28 ± 0.04 (5.31)	8.54 ± 0.14 (2.87)
Compound 4	7.25 ± 0.06 (56.6)	8.38 ± 0.17 (4.16)

Values represent the mean ± SEM of at least three individual experiments, performed in duplicate.
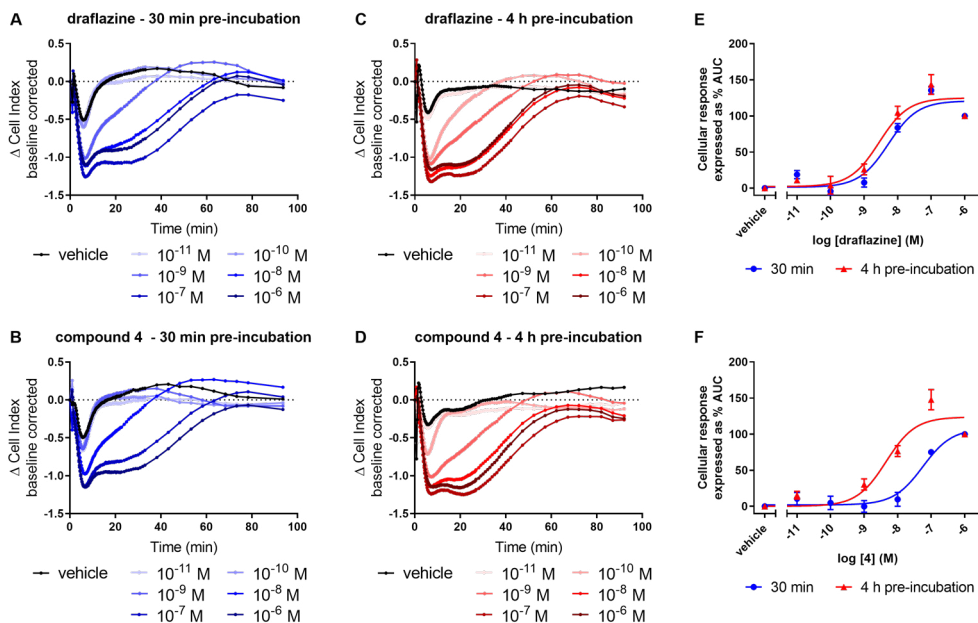
Figure 6: Functional characterization of draflazine and compound 4 on hENT1 endogenously expressed on U-2 OS cells. Cells were pre-incubated for 30 minutes or 4 hours and subsequently stimulated with $10^{-4.5}$ M adenosine. Concentration-dependent effects of draflazine (A,C) and compound 4 (B, D) after 30 minutes (A, B) and 4 hours (C, D) of pre-incubation, where representative xCELLigence traces of baseline-corrected adenosine responses are shown. Concentration-response curves of draflazine (E) and compound 4 (F) derived from corresponding AUCs up to 90 minutes after adenosine addition. Data shown are mean ± SEM from at least three separate experiments performed in duplicate.

Discussion

Affinity and potency have been and currently still are the main parameters investigated during *in vitro* drug discovery programs. However, during the last decade the importance of ligand binding kinetics has been highlighted by several studies[13,16]. The determination of the association and dissociation rate constant of a ligand to and from its target, in addition to residence time, has become the topic of many studies for various targets, such as G protein-coupled receptors (GPCRs)[28], kinases[29], ion channels[30] and other proteins[31]. In order to better understand the mechanism of action of ENT1 inhibitors, and to develop novel ones, it is essential to examine their binding kinetic parameters too[32]. Hence, in this study we focused on determining the affinity and binding kinetic parameters of reference ENT1 inhibitors

including draflazine, as well as a number of draflazine analogues.

A radioligand binding assay was used to determine the equilibrium affinity of all inhibitors. The affinities reported in our study are in line with the literature reports, where the affinity and/or the anti-aggregation effect of the reference compounds (NBTI, dilazep, dipyridamole and draflazine)[18,33,34] and compounds **1**, **3**, **5**, **6** and **9**[35-37]. Moreover, we found that for all inhibitors a Hill slope of -1 was preferred, indicating that the ligands are competing for the same binding site as [³H]NBTI. This finding is substantiated by the recently published crystal structure of ENT1 that indicates a commonly shared orthosteric binding site for NBTI and dilazep[7]. This binding site is then probably also targeted by dipyridamole, draflazine and its analogues.

The binding kinetics of the ENT1 inhibitors were evaluated with a competition association assay, which is based on the Motulsky-Mahan model that determines the time-dependent binding of two competing ligands[26]. As draflazine showed the longest RT of the reference ENT1 inhibitors, the draflazine scaffold was selected for further investigation of binding kinetic parameters (Tables 1 and 2). The association rate constants of the investigated analogues showed a small range of about one log unit, making correlations feeble. However, association rate constants should not be overlooked during drug optimization, when taking the disease of interest into consideration. For an acute disease, a fast association is required as an immediate response is vital[38]. In case of a chronic disease, k_{off} may seem of higher importance due to the long lasting effect needed, yet k_{on} is also of essence as the drug may need to compete with high concentrations of endogenous ligand under pathophysiological conditions[15]. In this study, we found that k_{off} and thus RT of the examined compounds ranged over two log units, from 6.2 minutes (**1**) up to 628 minutes (compound **4**), while their affinities were less divergent (Table 2). This broad range in k_{off} values is of interest when the concept of kinetic selectivity is also taken into account. As reviewed by Tonge[16], compounds with similar pK_i affinities for multiple targets (absence of thermodynamic selectivity) could still demonstrate kinetic selectivity for a target, which has been shown for muscarinic M3 receptors[39,40], LpxC enzyme[41] and cyclin-dependent kinases 2 and 9[42]. Although dilazep and dipyridamole are marketed drugs targeting ENT1, they are known to bind multiple targets, such as ENT2[43] and phosphodiesterases (PDE) 5, 6, 8, 10, 11[44]. As a result, a compound with high affinity and a long RT, such as the draflazine analogue compound **4** deserves further investigation. Actually, draflazine itself might for that reason be of less interest, although it was heavily investigated in clinical studies for unstable coronary disease[45] and *in vivo* animal studies on ischemic arrhythmias[46], for example.

Investigation of the correlations between equilibrium (pK_i) and kinetic (pK_D) affinity (Figure 5A) revealed a weak correlation between the two parameters. Only once the long RT inhibitor (**4**) was excluded, the two parameters were well correlated. Excluding compound **4** was supported by the fact that the equilibrium affinity, pK_i, was determined during a one hour assay, in which compounds with long RT had not yet reached equilibrium (Table 2, Figure 3B), resulting in the measurement

of an apparent and underestimated affinity. In addition, examination of binding kinetic parameters along with the "real" kinetic affinity revealed that affinity for the compounds of this study on ENT1 is driven by the dissociation rate constant (Figure 5B, C). In the past years, correlations have been performed between binding kinetic parameters and affinity in many studies and for multiple targets, like GPCRs and ion channels. In the case of neurokinin 1 (NK1) receptor, both dissociation and association rates of endogenous agonists correlated well with affinity[32], while for the binding to metabotropic glutamate 2 (mGlu$_2$) receptor or to K$_v$11.1 ion channel, only the k_{on} was the determinant parameter for affinity[30,47]. When the cannabinoid receptor type-2 (CB2) agonists where investigated, only the k_{off} was driving force for affinity[48]. From the plethora of data available, it has been shown that these correlations are target-specific and therefore could not have been hypothesized in advance[49].

Furthermore, washout radioligand experiments were performed to provide further insight in the binding kinetics and validate that the determined RT for compound **4** is a result of a long-lasting complex of the compound with the transporter and not of rebinding. The latter phenomenon is described as the renewed binding of recently dissociated ligands originating from the local environment of the target[16,50]. These high concentrations in the micro-environment could result in a long "overall"/apparent RT of a compound by consecutive binding to its initial target or those nearby[51]. However, the persistent binding of ENT1 by compound **4** after intensive washout, hence removal of the free inhibitor from the system, supports that the long-lasting complex of the compound with the transporter is due to long RT and not rebinding.

Next to binding parameters, the potency of selected inhibitors was studied, in order to investigate any possible correlation between binding kinetic parameters and functional efficacy. Here we used a recently developed real-time label-free assay to study ENT1 inhibition[24]. This assay is an indirect functional assay that measures the changes in adenosine receptor signaling resulting from ENT1 inhibition. In short, U-2 OS cells, endogenously expresses ENT1 and adenosine receptors (mainly A$_{2B}$) were pre-treated with the ENT1 inhibitors and subsequently treated with adenosine. In case of a potent inhibitor, high levels of ENT1 inhibition would be achieved, resulting in a significantly elevated extracellular concentration of adenosine, hence increased adenosine receptor signaling. Likewise, a weak ENT1 inhibitor would allow the translocation of adenosine intracellularly, leading to a lower extracellular concentration of adenosine and thus less adenosine receptor signaling. Thus, this assay simulates the physiologically relevant outcome of ENT1 inhibition, *i.e.* the modulation of the extracellular concentration of adenosine. As NBTI, dilazep and dipyridamole have been studied previously in this assay[24], we here examined the potency of a fourth reference inhibitor, draflazine, and its longest RT analogue, compound **4** (Table 2). A time-dependent effect was observed for the long RT inhibitor compound **4**, as its potency increased after a longer pre-incubation with the transporter (Table 3 and Figure 4). Taken together, the shift in potency of compound **4** indicates that ligand binding kinetics is a good predictor of *in vivo* target occupancy. Noteworthy, a typically used 30 min pre-incubation time with the inhibitors resulted

in IC_{50} values (Table 3) that were similar to the pK_i values determined by equilibrium radioligand binding assays (Table 2), while 4h pre-incubation resulted in IC_{50} values similar to the "real" affinities calculated based on the kinetic characteristics (K_D) of the compounds (Table 2). In other words, by not taking the kinetic aspects of ligand-target binding of long RT compounds into account (either by performing kinetic binding assays or by increasing incubation times in functional assays), the resulting (improved) pharmacological effect will be missed. Thus, the study of binding kinetics during a drug discovery project is of essence. Nevertheless, there are multiple pharmacological parameters that contribute to a pharmacological and safety profile of a drug. Therefore in addition to affinity, potency and binding kinetics, other parameters such as bioavailability, toxicity, metabolism and pharmacokinetic clearance should still be investigated.

In conclusion, we have established and validated a competition association assay as a valuable tool to determine the binding kinetics of unlabeled ENT1 inhibitors. Four reference inhibitors for ENT1 were characterized for their affinity and binding kinetics, while 9 analogues of draflazine were kinetically profiled for the first time. k_{off} Values were shown to be correlated to affinity, revealing that target engagement of ENT1 inhibitors is governed by their dissociation rate constants. The study of two compounds with distinct binding kinetics in a non-equilibrium functional assay demonstrated that a longer target-inhibitor complex is correlated to an increased functional effect, underlining an increased target occupancy for long RT inhibitors.

All in all, this is the first study where SKR are drawn in addition to SAR for ENT1 inhibitors, and relate inhibitors' binding kinetics to their functional effect. Hence, this study may inspire the incorporation of binding kinetics in the research and development of ENT1 inhibitors and likewise for other transport proteins.

Methods and Materials

Materials and Reagent

NBTI was purchased from SigmaAldrich (St. Louis, MO, USA) and dilazep was acquired from Asta-Werke (Degussa Pharma Gruppe, Bielefeld, Germany). Dipyridamole was kindly provided by Boehringer Ingelheim (Ingelheim, Germany), and draflazine and draflazine analogues were kindly gifted by Janssen Pharmaceutics (Beerse, Belgium). The radioligand [³H]-S-(4-Nitrobenzyl)-6-thioinosine ([³H]NBTI) with a specific activity of 50 Ci × mmol⁻¹ was purchased from PerkinElmer (Groningen, The Netherlands). Bovine serum albumin (BSA) and the bicinchoninic acid (BCA) protein assay kit were purchased from Fisher Scientific (Hampton, New Hampshire, United States), while 3-[(3-cholamidopropyl) dimethylammonio]-1-propanesulfonate (CHAPS) was obtained from Carl Roth GmbH (Karlsruhe, Germany). Erythrocytes were obtained from Sanquin Bloedvoorziening (Amsterdam, the Netherlands).

Dulbecco's modified Eagle's medium (DMEM) and Glutamax-1 were from Sigma Aldrich (St. Louis, MO, USA). Penicillin and streptomycin, were obtained from Duchefa Biochemie (Haarlem, The Netherlands). New Born Calf Serum (NBCS) was from Biowest (Nuaillé, France). Homo sapiens bone osteosarcoma cells (U-2 OS) were a kind gift from Mr. Hans den Dulk (Leiden Institute of Chemistry, department of Molecular Physiology, Leiden University, the Netherlands; originally obtained from and certified by American Type Culture Collection (ATCC)). All other chemicals and materials were obtained from standard commercial sources.

Cell culture

U-2 OS cells were cultured in DMEM supplemented with stable glutamine, 10% (v/v) NBCS, 100 IU/ml penicillin and 100 mg/ml streptomycin at 37 °C and 7% CO2. Cells were cultured as a monolayer on 10 cm ø plates and were subcultured twice every week at a ratio of 1:8. The cells were used for whole cell experiments when a confluency of ~ 90% was reached.

Membrane preparation

Erythrocytes stored at 4 °C in saline-adenine-glucose-mannitol (SAGM) were stirred in lysis buffer (10 mM $MgCl_2$ in 10 mM Tris-HCl, pH 8.0) (1/2 v/v) for 1h at 25 °C and homogenized using an Ultra Turrax homogenizer at 24,000 rpm (IKAWerke GmbH & Co.KG, Staufen, Germany). The homogenized sample was centrifuged at 8000 rpm (13700 g) at 4 °C for 1 h in a Sorvall RC 6+ centrifuge (Thermo Scientific). Pellets were resuspended in ice-cold milli-Q water (Millipore S.A.S., Molsheim, France) homogenized and centrifuged at 37,500 rpm (150,000 g) at 4°C for 20 min in an Optima LE80 K ultracentrifuge (Beckman Coulter, Fullerton, CA). After resuspension of pellets in ice-cold milli-Q water, the centrifugation and homogenization steps were repeated till the supernatant was colorless. After the last centrifugation step, pellet was resuspended in buffer (50 mM Tris-HCl, pH 7.4 at 4 °C) and homogenized. Aliquots were prepared and stored at -80 °C. Membrane protein concentrations were measured using the BCA method[19].

Radioligand binding assay

In all experiments, erythrocyte membranes were thawed, homogenized using an Ultra Turrax homogenizer at 24,000 rpm (IKA-Werke GmbH & Co.KG, Staufen, Germany) and diluted to the desired concentration (2 µg/well) using assay buffer (50 mM Tris-HCl pH 7.4, 0.1% (w/v) CHAPS). Assay buffer, (radio)ligands and membranes were cooled for 30 minutes at 10 °C prior to the experiment. Nonspecific binding was determined in the presence of 10^{-5} M unlabeled NBTI. Total reaction volume was 100 µL (except for wash-out experiments which was 400 µL) and dimethylsulfoxide

(DMSO) final concentrations were ≤0.25%. In all cases total binding did not exceed 10% of the [³H]NBTI added to the assay in order to prevent ligand depletion.

Equilibrium Assays

Displacement experiments were carried out using [³H]NBTI (4 nM) and a competing ligand at multiple concentrations. Binding was initiated by addition of membranes, and samples were incubated at 10 °C for 60 min to reach equilibrium. The incubation was terminated by rapid vacuum filtration over 96-well Whatman GF/C filter plates using a PerkinElmer Filtermate harvester (PerkinElmer, Groningen, Netherlands). Filters were subsequently washed ten times using ice-cold wash buffer (50 mM Tris-HCl, pH 7.4). Filter plates were dried at 55 °C for about 45 min and afterwards 25 µL Microscint (PerkinElmer) was added per well. Filter-bound radioactivity was determined by liquid scintillation spectrometry using a 2450 Microbeta² scintillation counter (PerkinElmer).

Saturation binding experiments were carried out by incubating increasing concentrations of [³H]NBTI (from 0.12 to 12 nM) with membrane aliquots for 60 min at 10 °C. Incubation was terminated by filtration and samples were obtained as described under "*Displacement experiments*".

Kinetic Assays

Association experiments were performed by incubation of [³H]NBTI (4 nM) with membrane aliquots at 10 °C. The amount of receptor-bound radioligand was determined after filtration at different time intervals for a total incubation time of 60 minutes and samples were obtained as described under "*Displacement experiments*".

Dissociation experiments were carried out by a 60 minute pre-incubation of radioligand [³H]NBTI (4 nM) and membrane aliquots. Subsequently, dissociation of the radioligand at different time points up to 150 minutes was initiated by addition of 5 µl NBTI (final concentration 10 µM). Dissociation experiments were performed at 10 °C. The amount of receptor-bound radioligand was determined after filtration and samples were obtained as described under "*Displacement experiments*".

Competition association experiments were performed by incubation of radioligand (4 nM) and competing ligand at its IC$_{50}$ concentration (*i.e.* determined in displacement experiments) with membrane aliquots at 10 °C. The amount of transporter-bound radioligand was determined at different time points up to 60 minutes, except for the case of compounds showing a RT longer than 60 minutes. In this case, the total time of measurement was extended up to 180 minutes. The amount of transporter-bound radioligand was determined after filtration at different time intervals and samples were obtained as described under "*Displacement experiments*".

Wash-out experiments were performed by incubating the competing ligands at a final concentration of 10 x IC_{50} (as determined in displacement experiments) with erythrocyte membranes for 1 h at 10 °C while gently shaking. Subsequently the samples were centrifuged at 13,200 rpm (16,100g) at 4 °C for 5 min and the supernatant containing the unbound ligand was removed. Pellets were resuspended in 1 mL of assay buffer, and samples were incubated for 10 min at 10 °C. The control (unwashed) samples were kept on ice during centrifugation and supernatant removal. After four centrifugation and washing cycles in total, supernatant was discarded and the membranes were resuspended in a total volume of 400 µL containing 4 nM [³H] NBTI. After 60 min incubation at 10 °C, incubations were terminated by rapid filtration through GF/C filters using a Brandel harvester (Brandel, Gaithersburg, MD). Filters were washed three times and collected in tubes. Emulsifier-Safe scintillation fluid (Perkin Elmer, Groningen, the Netherlands) was added and samples were counted by scintillation spectrometry using a Tri-carb 2900 TR liquid scintillation counter (Perkin Elmer, Boston, MA).

Impedance-based morphology assay

Detection principle

Impedance-based morphology assays were performed using the xCELLigence real-time cell analyser (RTCA) system[20,21], as described previously[22]. In short, the RTCA system measures the electrical impedance generated by cells adhering to gold-coated electrodes embedded on the bottom of microelectronic E-plates. Changes in impedance (Z) could result from variations in number, degree of adhesion, cellular viability and morphology of cells. These changes are recorded continuously at 10 kHz and displayed in the unitless parameter called Cell Index (CI)[21,23], which is defined (Z_i-Z_0) Ω /15 Ω. Z_i is the impedance at a given time point and Z_0 represents the baseline impedance in the absence of cells, which is measured prior to the start of the experiment.

Functional evaluation of pIC_{50} values for ENT1 inhibitors

The assay was used as previously described by Vlachodimou *et al.*[24]. In short, U-2 OS cells were harvested and centrifuged at 200x *g* (1500 rpm) for 5 min. Z_0 was measured after the addition of 40 µL culture media to 96 well PET E-plates (Bioké, Leiden). 20,000 cells were added in a volume of 50 µL per well. After resting at room temperature for at least 30 min, the E-plate was placed into the recording station situated in a 37°C and 5% CO_2 incubator. Impedance was measured every 15 minutes overnight. After 18 hours of recording, cells were pre-treated with increasing concentrations of ENT1 inhibitor or vehicle control (0.25% DMSO in Phosphate-buffered saline (PBS)) in 5 µL. CI was recorded for 30 minutes (recording schedule: 15 second intervals for 20 minutes, followed by 1 minute intervals for 10 minutes)

or 4 hours (recording schedule after 30 minutes: 5 minutes interval for 45 minutes, followed by 15 minutes intervals). Subsequently, cells were stimulated with $10^{-4.5}$ M adenosine or vehicle control (0.125% DMSO in PBS) in 5 μL and CI was recorded for at least 90 minutes with a recording schedule of 15 second intervals for 20 minutes, followed by intervals of 1 minute for 10 minutes and finally 5 minutes. In all cases, final well volumes and DMSO concentrations upon cell and ligands addition were 100 μL and 0.375%, respectively, for all wells.

Data analysis

Radioligand binding assays

Data analyses were performed using GraphPad Prism 8.1 software (GraphPad Software Inc., San Diego, CA, USA). K_D and B_{max} values were obtained from radioligand saturation assays by non-linear regression curve fitting using the one site: "total and non-specific binding" equation. pIC_{50} values were obtained from radioligand displacement assays by non-linear regression curve fitting into a sigmoidal concentration-response curve using the "log(inhibitor) vs. response" graphpad analysis equation. The data were fitted both in "log(inhibitor) vs. response (three parameters)" and "log(inhibitor) vs. response - Variable slope (four parameters)", and the two analysis were compared. In all cases the former analysis was preferred where the Hill-slope is fixed at -1.0, showing competitive binding. Hence, pK_i values were calculated from pIC_{50} values and the saturation K_D value via the ChengPrusoff equation[25]: $K_i = IC_{50} / (1 + [radioligand] / K_D)$.

The dissociation rate constant k_{off} was obtained using a one-phase exponential decay analysis of data from a radioligand dissociation assay. Association rate constant k_{on} was determined using the equation: $k_{on} = (k_{obs} - k_{off}) / [radioligand]$, in which L is the concentration of radioligand and k_{obs} was determined using a one phase association analysis of data from a radioligand association assay. The association and dissociation rates were used to calculate the kinetic K_D using: $K_D = k_{off} / k_{on}$

Association and dissociation rate constants for unlabelled ENT1 inhibitors were determined by non-linear regression analysis of competition association data as described by Motulsky and Mahan[26]. The kinetics of competitive binding analysis of GraphPad Prism software was used, where k_1 and k_2 are the k_{on} ($M^{-1}min^{-1}$) and k_{off} (min^{-1}) of [^{3}H]NBTI obtained from radioligand association and dissociation assays, respectively, L is the radioligand concentration (nM), I is the concentration of unlabeled competitor (nM), X is the time (min) and Y is the specific binding of the radioligand (DPM). Fixing these parameters allows the following parameters to be calculated: k_3, which is the k_{on} value ($M^{-1}min^{-1}$) of the unlabeled ligand; k_4, which is the k_{off} value (min^{-1}) of the unlabeled ligand and B_{max}, that equals the total binding (DPM). All competition association data were globally fitted. The residence time (RT) was calculated using: RT = 1 / k_{off} [27].

cLogP values were calculated using ChemDraw Professional 16.0. All data are shown as mean ± S.E.M. of at least three independent experiments performed in duplicate. Statistical analysis was performed if indicated, using a parametric paired Student's t test (ns p>0.05, * p ≤ 0.05, ** p ≤ 0.01, *** p ≤ 0.001, **** p ≤ 0.0001).

Label-free whole-cell assay

RTCA software 2.0 (ACEA Biosciences, Inc.) was used to capture the experimental data. All data were analyzed using GraphPad Prism 8.1 (GraphPad software, San Diego, CA, USA). Ligand responses, baseline-corrected to vehicle control, were normalized at the time of ligand addition to obtain Δ Cell Index (Δ CI) values to correct for ligand-independent responses. The time of normalization was either at approximately 18 h 30 min or at 22 h after cell seeding for analysis of adenosine effect (depending on the pre-incubation time of the inhibitors, *i.e.* 30 min or 4 h).

The absolute values of Total Area Under the Curve (AUC) up to 90 min after adenosine addition were exported to Graphpad Prism for further analysis yielding concentration–response curves. pIC_{50} values of ENT1 inhibitors (Table 3) were obtained using non-linear regression curve fitting of Total AUC data into a sigmoidal dose-response curve as described by "log(inhibitor) vs. response (three parameters)" analysis of graphpad prism software. Data shown are the mean ± SEM of at least three individual experiments performed in duplicate.

Acknowledgements

References

1   Pastor-Anglada, M. & Pérez-Torras, S. Emerging Roles of Nucleoside Transporters. *Frontiers in Pharmacology* **9**, doi:10.3389/fphar.2018.00606 (2018).

2   Illes, P., Klotz, K.-N. & Lohse, M. J. Signaling by extracellular nucleotides and nucleosides. *Naunyn-Schmiedeberg's Archives of Pharmacology* **362**, 295-298, doi:10.1007/s002100000308 (2000).

3   Berg, J. M., Tymoczko, J. L. & Stryer, L. *Biochemistry*. 7th edn, (W. H. Freeman and Company, 2012).

4   Pastor-Anglada, M. & Pérez-Torras, S. Who Is Who in Adenosine Transport. *Frontiers in pharmacology* **9**, 627-627, doi:10.3389/fphar.2018.00627 (2018).

5   Boswell-Casteel, R. C. & Hays, F. A. Equilibrative nucleoside transporters-A review. *Nucleosides, nucleotides & nucleic acids* **36**, 7-30, doi:10.1080/152577 70.2016.1210805 (2017).

6   Jennings, L. L. *et al.* Distinct regional distribution of human equilibrative nucleoside transporter proteins 1 and 2 (hENT1 and hENT2) in the central nervous system. *Neuropharmacology* **40**, 722-731, doi:https://doi.org/10.1016/S0028-3908(00)00207-0 (2001).

7   Wright, N. J. & Lee, S.-Y. Structures of human ENT1 in complex with adenosine reuptake inhibitors. *Nature Structural & Molecular Biology* **26**, 599-606, doi:10.1038/s41594-019-0245-7 (2019).

8   Mackey, J. R. *et al.* Functional nucleoside transporters are required for gemcitabine influx and manifestation of toxicity in cancer cell lines. *Cancer Res* **58**, 4349-4357 (1998).

9   Iikura, M. *et al.* ENT1, a ribavirin transporter, plays a pivotal role in antiviral efficacy of ribavirin in a hepatitis C virus replication cell system. *Antimicrobial agents and chemotherapy* **56**, 1407-1413, doi:10.1128/AAC.05762-11 (2012).

10   Van Belle, H. Myocardial protection by nucleoside transport inhibition. *Transplant Proc* **27**, 2804-2805 (1995).

11   Khalil, A., Belal, F. & Al-Badr, A. A. Dipyridamole: comprehensive profile. *Profiles Drug Subst Excip Relat Methodol* **31**, 215-280, doi:10.1016/s0099-5428(04)31007-5 (2005).

12   Deguchi, H. *et al.* Dilazep, an antiplatelet agent, inhibits tissue factor expression in endothelial cells and monocytes. *Blood* **90**, 2345-2356 (1997).

13   Copeland, R. A. The drug–target residence time model: a 10-year retrospective. *Nature Reviews Drug Discovery* **15**, 87, doi:10.1038/nrd.2015.18 (2015).

14   Swinney, D. C. The role of binding kinetics in therapeutically useful drug action. *Curr Opin Drug Discov Devel* **12**, 31-39 (2009).

15   de Witte, W. E. A., Danhof, M., van der Graaf, P. H. & de Lange, E. C. M. In vivo Target Residence Time and Kinetic Selectivity: The Association Rate Constant as Determinant. *Trends Pharmacol Sci* **37**, 831-842, doi:10.1016/j.tips.2016.06.008 (2016).

16   Tonge, P. J. Drug-Target Kinetics in Drug Discovery. *ACS chemical neuroscience* **9**, 29-39, doi:10.1021/acschemneuro.7b00185 (2017).

17   Lu, H. & Tonge, P. J. Drug-target residence time: critical information for lead optimization. *Current opinion in chemical biology* **14**, 467-474, doi:10.1016/j.cbpa.2010.06.176 (2010).

18   Rehan, S., Ashok, Y., Nanekar, R. & Jaakola, V. P. Thermodynamics and kinetics of inhibitor binding to human equilibrative nucleoside transporter subtype-1. *Biochem Pharmacol* **98**, 681-689, doi:10.1016/j.bcp.2015.09.019 (2015).

19   Smith, P. K. *et al.* Measurement of protein using bicinchoninic acid. *Anal Biochem*

150, 76-85 (1985).

20 Xi, B., Yu, N., Wang, X., Xu, X. & Abassi, Y. A. The application of cell-based label-free technology in drug discovery. *Biotechnol J* **3**, 484-495, doi:10.1002/biot.200800020 (2008).

21 Yu, N. *et al.* Real-Time Monitoring of Morphological Changes in Living Cells by Electronic Cell Sensor Arrays: An Approach To Study G Protein-Coupled Receptors. *Analytical Chemistry* **78**, 35-43, doi:10.1021/ac051695v (2006).

22 Hillger, J. M. *et al.* Whole-cell biosensor for label-free detection of GPCR-mediated drug responses in personal cell lines. *Biosensors and Bioelectronics* **74**, 233-242, doi:https://doi.org/10.1016/j.bios.2015.06.031 (2015).

23 Fang, Y. The development of label-free cellular assays for drug discovery. *Expert Opinion on Drug Discovery* **6**, 1285-1298, doi:10.1517/17460441.2012.642360 (2011).

24 Vlachodimou, A., IJzerman, A. P. & Heitman, L. H. Label-free detection of transporter activity via GPCR signalling in living cells: A case for SLC29A1, the equilibrative nucleoside transporter 1. *Scientific Reports* **9**, 13802, doi:10.1038/s41598-019-48829-3 (2019).

25 Cheng, Y. & Prusoff, W. H. Relationship between the inhibition constant (KI) and the concentration of inhibitor which causes 50 per cent inhibition (I50) of an enzymatic reaction. *Biochemical Pharmacology* **22**, 3099-3108, doi:https://doi.org/10.1016/0006-2952(73)90196-2 (1973).

26 Motulsky, H. J. & Mahan, L. C. The kinetics of competitive radioligand binding predicted by the law of mass action. *Mol Pharmacol* **25**, 1-9 (1984).

27 Copeland, R. A. Evaluation of enzyme inhibitors in drug discovery. A guide for medicinal chemists and pharmacologists. *Methods Biochem Anal* **46**, 1-265 (2005).

28 Sykes, D. A., Stoddart, L. A., Kilpatrick, L. E. & Hill, S. J. Binding kinetics of ligands acting at GPCRs. *Molecular and Cellular Endocrinology* **485**, 9-19, doi:https://doi.org/10.1016/j.mce.2019.01.018 (2019).

29 Bradshaw, J. M. *et al.* Prolonged and tunable residence time using reversible covalent kinase inhibitors. *Nat Chem Biol* **11**, 525-531, doi:10.1038/nchembio.1817 (2015).

30 Yu, Z. *et al.* Structure–Affinity Relationships (SARs) and Structure–Kinetics Relationships (SKRs) of Kv11.1 Blockers. *Journal of Medicinal Chemistry* **58**, 5916-5929, doi:10.1021/acs.jmedchem.5b00518 (2015).

31 Costa, B. *et al.* TSPO ligand residence time: a new parameter to predict compound neurosteroidogenic efficacy. *Scientific Reports* **6**, 18164, doi:10.1038/srep18164 (2016).

32 Nederpelt, I., Bleeker, D., Tuijt, B., IJzerman, A. P. & Heitman, L. H. Kinetic binding and activation profiles of endogenous tachykinins targeting the NK1 receptor. *Biochem Pharmacol* **118**, 88-95, doi:10.1016/j.bcp.2016.08.004 (2016).

33   Gupte, A. *et al.* 6-Benzylthioinosine analogues: Promising anti-toxoplasmic agents as inhibitors of the mammalian nucleoside transporter ENT1 (es). *Biochemical Pharmacology* **71**, 69-73, doi:https://doi.org/10.1016/j.bcp.2005.10.031 (2005).

34   SenGupta, D. J. & Unadkat, J. D. Glycine 154 of the equilibrative nucleoside transporter, hENT1, is important for nucleoside transport and for conferring sensitivity to the inhibitors nitrobenzylthioinosine, dipyridamole, and dilazep. *Biochem Pharmacol* **67**, 453-458, doi:10.1016/j.bcp.2003.09.018 (2004).

35   Beukers, M. W., Kerkhof, C. J., IJzerman, A. P. & Soudijn, W. Nucleoside transport inhibition and platelet aggregation in human blood: R75231 and its enantiomers, draflazine and R88016. *Eur J Pharmacol* **266**, 57-62 (1994).

36   IJzerman, A. P., Thedinga, K. H., Custers, A. F., Hoos, B. & Van Belle, H. Inhibition of nucleoside transport by a new series of compounds related to lidoflazine and mioflazine. *Eur J Pharmacol* **172**, 273-281 (1989).

37   Hammond, J. R. Interaction of a series of draflazine analogues with equilibrative nucleoside transporters: species differences and transporter subtype selectivity. *Naunyn Schmiedebergs Arch Pharmacol* **361**, 373-382 (2000).

38   Smith, G. F. in *Progress in Medicinal Chemistry* Vol. 48 (eds G. Lawton & D. R. Witty) 1-29 (Elsevier, 2009).

39   Tautermann, C. S. *et al.* Molecular basis for the long duration of action and kinetic selectivity of tiotropium for the muscarinic M3 receptor. *J Med Chem* **56**, 8746-8756, doi:10.1021/jm401219y (2013).

40   Sykes, D. A. *et al.* The Influence of receptor kinetics on the onset and duration of action and the therapeutic index of NVA237 and tiotropium. *J Pharmacol Exp Ther* **343**, 520-528, doi:10.1124/jpet.112.194456 (2012).

41   Walkup, G. K. *et al.* Translating slow-binding inhibition kinetics into cellular and in vivo effects. *Nat Chem Biol* **11**, 416-423, doi:10.1038/nchembio.1796 (2015).

42   Ayaz, P. *et al.* Conformational Adaption May Explain the Slow Dissociation Kinetics of Roniciclib (BAY 1000394), a Type I CDK Inhibitor with Kinetic Selectivity for CDK2 and CDK9. *ACS Chemical Biology* **11**, 1710-1719, doi:10.1021/acschembio.6b00074 (2016).

43   Playa, H. *et al.* Dilazep analogues for the study of equilibrative nucleoside transporters 1 and 2 (ENT1 and ENT2). *Bioorg Med Chem Lett* **24**, 5801-5804, doi:10.1016/j.bmcl.2014.10.026 (2014).

44   Gillespie, P. G. & Beavo, J. A. Inhibition and stimulation of photoreceptor phosphodiesterases by dipyridamole and M&B 22,948. *Mol Pharmacol* **36**, 773-781 (1989).

45   Andersen, K., Dellborg, M. & Swedberg, K. Nucleoside transport inhibition by draflazine in unstable coronary disease. *European Journal of Clinical Pharmacology* **51**, 7-13, doi:10.1007/s002280050153 (1996).

46   Wainwright, C. L., Parratt, J. R. & Van Belle, H. The antiarrhythmic effects of the nucleoside transporter inhibitor, R75231, in anaesthetized pigs. *Br J Pharmacol* **109**, 592-599, doi:10.1111/j.1476-5381.1993.tb13612.x (1993).

47 Doornbos, M. L. J. *et al.* Impact of allosteric modulation: Exploring the binding kinetics of glutamate and other orthosteric ligands of the metabotropic glutamate receptor 2. *Biochemical Pharmacology* **155**, 356-365, doi:https://doi.org/10.1016/j.bcp.2018.07.014 (2018).

48 Soethoudt, M. *et al.* Structure-kinetic relationship studies of cannabinoid CB2 receptor agonists reveal substituent-specific lipophilic effects on residence time. *Biochemical Pharmacology* **152**, 129-142, doi:https://doi.org/10.1016/j.bcp.2018.03.018 (2018).

49 Doornbos, M. L. J. *et al.* Discovery and Kinetic Profiling of 7-Aryl-1,2,4-triazolo[4,3-a]pyridines: Positive Allosteric Modulators of the Metabotropic Glutamate Receptor 2. *J Med Chem* **60**, 6704-6720, doi:10.1021/acs.jmedchem.7b00669 (2017).

50 Vauquelin, G. & Charlton, S. J. Long-lasting target binding and rebinding as mechanisms to prolong in vivo drug action. *Br J Pharmacol* **161**, 488-508, doi:10.1111/j.1476-5381.2010.00936.x (2010).

51 Vauquelin, G. On the 'micro'-pharmacodynamic and pharmacokinetic mechanisms that contribute to long-lasting drug action. *Expert Opin Drug Discov* **10**, 1085-1098, doi:10.1517/17460441.2015.1067196 (2015).